

Magnetic Nanocomposite Materials for RFID and RF Passives Miniaturization

Lara Martin¹, #Daniela Staiculescu², Haiying Li¹, S.L. Ooi¹, C. P. Wong², M.M. Tentzeris²

¹Motorola, Plantation, FL, 33322, U.S.A.

²Georgia Institute of Technology, Atlanta, GA, 30332, U.S.A.

1. Introduction

The inception of RFID (radio frequency identification) has enabled contactless transfer of information without the requirement of line of sight association, specifically between a reader and transponders that reside on an identified item. As the technology for RFID systems developed, there has been a need to design more flexible systems enabled at the transponder, namely miniaturization of the transponder and ability to tune system performance to accommodate EM (electromagnetic) absorption and interference from surrounding media [1]. Three-dimensional transponder antennas that utilize wound coil inductors do make use of magnetic cores, but magnetic materials for two-dimensional embedded planar antennas have not yet been successfully realized for standard use. As their three-dimensional counterparts, two-dimensional embedded antennas can reap the same benefits from magnetic materials.

One of the most significant challenges for applying new magnetic materials is understanding the interrelationships of the new materials, design, and performance. In previous studies, it can often be cited that the objectives of miniaturization and improved performance are limited by the limited availability of materials that possess the required properties [2]. Recently, formulation of nano-size ferrite particles has been reported [3] and formulation of magnetic nanocomposites comprised of ferrite filler and organic matrix has been demonstrated [4].

In this study, a benchmark structure is first designed in an EM simulator with the assumptions for an unfilled silicone substrate, followed by physical realizing and testing the structure to ensure agreement with simulation. Then, the EM simulator results, which assume material property variables of a magnetic nanocomposite and geometric design variables, are incorporated into the Design of Experiments (DOE) and Response Surface Method (RSM) statistical optimization techniques, which give a thorough understanding of the system and, most importantly, give information such as how the electrical performance is affected and how they could enhance the capability for miniaturization. Previous work [5] shows successful use of hybrid statistical techniques in microwave system analysis and optimization, but this is the first reported work on incorporating the material properties into the design process. This methodology enables the designer to investigate a system of parameters that include material properties and design geometries for the structure simultaneously and weigh tradeoffs instantaneously, thereby developing an in-depth understanding of the implications that new materials have on design.

2. Benchmarking structure

Without loss of generality, the choice of the benchmarking structure was a short-circuited quarter-wavelength rectangular patch antenna for RFID UHF band (400 – 930 MHz). The initial structure was designed for the lower end of the UHF spectrum and was modeled using HFSS full wave EM (electromagnetic) software. The initial substrate was pure silicone ($\epsilon_r = 2.65$ and $\tan\delta_\mu = 0.001$) of 1.6 mm thickness, and the structure showed a resonant frequency of 385 MHz for a 110mm x 110 mm short-circuited patch dimension.

To begin the optimization, the hybrid EM simulation/statistical tools methodology was applied to quantify the effect of material properties and geometries on the performance of the benchmarking structure. The chosen statistical tool was full factorial DOE with center points [6]. The factorial

designs are used in experiments involving several factors, where the goal is the study of the joint effects of the factors on a response. The 2^k factorial design is the simplest one, with k factors at 2 levels each. It provides the smallest number of runs for studying k factors and is widely used in factor screening experiments [6]. Center points are defined at the center of the design space and increase the capability of investigating the validity of the model, including curvature in the response and accounting for variation in the fabrication process of the structure. Since the statistical models are based on deterministic simulations, the variation of the center points was statistically simulated. Specifically, center points were randomly generated assuming a mean equal to the exact center point value and variation expected in a typical fabrication process. For the expected variations, 3σ fabrication processes were assumed for stated tolerance capabilities.

For the DOE, the parameters under investigation as input variables were ϵ_r (relative permittivity), μ_r (relative permeability) and d (inset length). Although not included as an input for the initial DOE, w (microstrip width) was simulated separately to ensure 50Ω impedance matching, depending on values for ϵ_r , μ_r , and h for the different experimental conditions. The antenna dimensions included as input variables are shown in Fig. 1, with $h = 0.2\text{mm}$.

The design space for the input variables was chosen such that it includes values of an actual magnetic nanocomposite material that has been formulated and incorporates fabrication limitations and design rules for the dimensions. The ranges for the input variables for the initial DOE are presented in Table 1 and the tolerance capabilities used to simulate center point variability are as follows: ± 0.15 for ϵ_r and μ_r and ± 0.3 mm for d . The output variables, or responses, for the DOE were the resonant frequency f_{res} and the corresponding return loss RL .

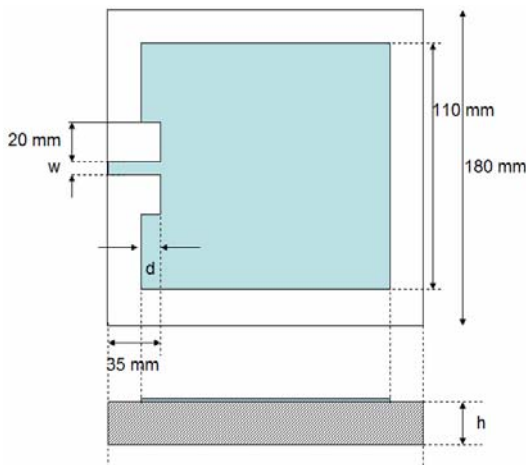


Fig. 1. Antenna dimensions

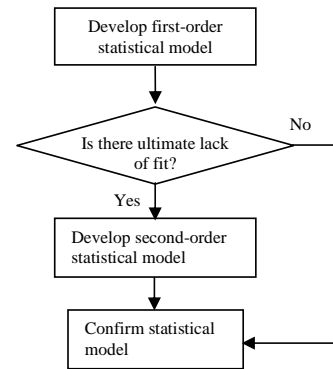


Fig. 2. Methodology used for optimization

Variable	Low value “-”	High value “+”	Center point
ϵ_r	2.5	6.5	4.5
μ_r	1	6.5	3.75
d (mm)	3	9	6

Table 1. Ranges for the input variables.

Once the responses were obtained for the experiment, the best fitting first order statistical model was determined. Next, the fit was investigated for ultimate lack of fit. An ultimate lack of fit can arise from curvature in the response or increased variation of fit at one end of the model, for example. In cases that curvature in the response is detected, the analysis may be extended to additional axial points indicated by the RSM method, which can account for curvature through second order model development. Usually, these second order models are reasonable approximations of the true functional relationship over relatively small regions. Once validated

using statistical diagnostic tools, the models approximate the actual system within the defined design space. This methodology used for the optimization is presented as a flowchart in Fig. 2.

3. Statistical analysis

From the DOE, first order statistical models were developed. The first order model for f_{res} showed to have poor fit, and the first-order model for RL showed to have reasonable fit. Upon inspection of the statistical diagnostic tools used to validate assumptions of normality and equal variance, curvature was detected for f_{res} . Even with the detected curvature, the model for f_{res} was statistically significant at the 95% confidence level. The first order model for RL was also statistically significant at the 95% confidence level.

Continuing with the optimization methodology, a second order model was developed using RSM to account for the detected curvature in f_{res} [6]. The second order model for f_{res} was statistically significant at the 95% confidence level. The developed model included the terms ε_r , μ_r , and the interaction $\varepsilon_r * \mu_r$. The curvature was alleviated by including the second order terms ε_r^2 and μ_r^2 . Additionally, there was significant lack of fit at the 95% confidence level. Although the equal variance assumption could not be validated, the normality assumption was validated. The model for f_{res} is given by (1).

The developed statistical model for RL from the RSM included the term for d only. The model was further analyzed, and the assumptions of normality and equal variance were validated. Additionally, there was no significant lack of fit at the 95% confidence level. The model for RL is given by (2).

$$f_{res} = 147.8 - 26.5 \left(\frac{\varepsilon_r - 4.5}{1.5} \right) - 35.0 \left(\frac{\mu_r - 4.25}{1.75} \right) + 6.54 \left(\frac{\varepsilon_r - 4.5}{1.5} \right) \left(\frac{\mu_r - 4.25}{1.75} \right) + 5.78 \left(\frac{\varepsilon_r - 4.5}{1.5} \right)^2 + 11.38 \left(\frac{\mu_r - 4.25}{1.75} \right)^2 \quad (1)$$

$$RL = -14.72 + 2.77 \left(\frac{d - 6}{2} \right) \quad (2)$$

Before accepting (1) and (2) as the final models, the models had to be confirmed. The confirmations of the models were performed for the following combination of parameters: $\varepsilon_r = 5.1$, $\mu_r = 2.9$, and $d = 4.7$ mm. This combination of input variables was simulated in the EM simulator and was also predicted with the developed models. The results of the simulation compared to the 95% confidence intervals defined by the lower and upper bounds for the predicted f_{res} and RL are as follows: for f_{res} , the confidence interval is between 160.2 and 179.6 MHz and the simulated value is 171.4 MHz, while for the RL the interval is between -22.1 and -11.0 dB and the simulated value is -14.5 dB. Because the simulation values fall into the 95% confidence intervals, the models were confirmed. With this confirmation, the models given by (1)-(2) were accepted as the final models.

4. Model interpretation and application

The final step in the study was applying measurements of a fabricated magnetic nanocomposite material to the models. The material was formulated from Dow Corning Sylgard 184 silicone and Steward NiZn ferrite powder #72599. A 40 vol% ferrite paste was produced with a mixer at 240 rpm and 110°C for 30 minutes. The paste was transferred into a flat mold and vacuum cured with a hold confirmed to occur at >125°C for 50 minutes to produce a 1.6 mm thick substrate.

The material was measured using an HP4291A impedance analyzer with material fixtures 16453A for ε_r and 16454A for μ_r . There were 5 measurements taken for each ε_r and μ_r . The summary statistics including the mean and 95% C.I. (confidence intervals) for ε_r and μ_r are given in Table 2. Based on these results, the values used in the model were $\varepsilon_r = 6.3$ and $\mu_r = 4.4$.

According to the model, RL is minimized when d is minimized. To minimize RL , d was set equal to 4. With these values for ϵ_r , μ_r , and d , the model predicted $f_{res} = 122$ MHz and $RL = -17.5$ dB. The surfaces of the possible solutions from the statistical models are shown in Fig. 3.

Comparing substrates, the shift down in frequency from $f_{res} = 385$ MHz for the pure silicone substrate to 122 MHz for the magnetic nanocomposite substrate proves the miniaturization concept (by a factor $385/122 \sim 3.2$). Similar benefits can be observed for other large-size RF passives, such as integrated RF inductors, that potentially play a critical role in the size of integrated RF modules.

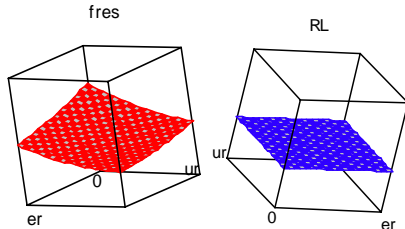


Fig. 3. Surfaces of possible solutions for optimized f_{res} and RL

	mean	Lower CI	Upper CI
ϵ_r	6.332	6.227	6.437
μ_r	4.252	4.249	4.255

Table 2. Mean and 95% confidence intervals for ϵ_r and μ_r

5. Conclusions

A combination of electromagnetic and statistical tools (DOE and RSM) has been used to investigate the impact of magnetic nanocomposite materials to the miniaturization of RFID antennas and RF passives considering geometric, material and fabrication parameters and uncertainties. This approach has been applied to the design of a benchmarking microstrip patch antenna and has enabled the assessment of implications that materials have on this design. The experiment was simple to implement and provided a thorough understanding of the issues to be confronted in the design process. The statistical analysis provided equations to quantify the effect of material properties on the electrical figures of merit, which can relate to the capability for miniaturization. By extending this approach to carefully investigate the behavior of a complete module and package and including additional parameters, such as the overall structure size and the material loss variation with frequency, the designer can save a lot of time, shorten the design cycle of added functions, and optimize designs in a simple and elegant manner and with a profound understanding of how all these aspects are affecting each other. In addition, this approach could provide a very simple way to determine a-priori confidence levels for component and system performance considering variations of fabrication processes and uncertainties/tolerances in the characterization of exotic novel materials, such as nanocomposites.

References

- [1] "Magnetic Materials for RFID," TechnoForum 2005, TDK, http://www.tdk.co.jp/tf2005/pdf_e/2f0215e.pdf.
- [2] N. Das and A. K. Ray, "Magneto Optical Technique for Beam Steering by Ferrite Based Patch Arrays," *IEEE Transactions on Antennas and Propagation*, vol. 49, no. 8, August (2001); pp. 1239-1241.
- [3] S. Morrison, C. Cahill, E. Carpenter, S. Calvin, R. Swaminathan, M. McHenry, V. Harris, "Magnetic and Structural Properties of Nickel Zinc Ferrite Nanoparticles Synthesized at Room Temperature," *Journal of Applied Physics*, vol. 95, no. 11, June (2004); pp. 6392-6395.
- [4] H. Dong, F. Liu, Q. Song, Z.J. Zhang, C. P. Wong, "Magnetic Nanocomposite for High Q Embedded Inductor," *IEEE International Symposium and Exhibition on Advance Packaging Materials: Process, Properties, and Interfaces*, Atlanta, Georgia, March (2004); pp. 171-174.
- [5] C. You, D. Staiculescu, L. Martin, W. Hwang, M. M. Tentzeris, "Efficient Co-design of Composite Smart Structures (Antennas and Mechanical Structures) Using a Novel Hybrid Optimization Technique," *IEEE Antennas and Propagation Society International Symposium*, San Francisco, California, June (2006); pp. 569-572.
- [6] J. Neter *et al*, "Applied Linear Statistical Models", 4th Ed., The McGraw-Hill Companies, Chicago, 1996.